Passive drag control of a turbulent wake by local disturbances

O. Cadot, B. Thiria and J.-F. Beaudoin[1]

Unité de Mécanique de l'Ecole Nationale Supérieure de Techniques Avancées, Chemin de la Hunière, 91761 Palaiseau cedex, France.

[1] *Department of Research and Innovation, PSA Peugeot-Citroën, 2 route de Gisy, 78943 Vélizy-Villacoublay, France.*

Abstract. Global properties such as recirculation bubble, shedding frequency, base pressure and global mode amplitude of a turbulent wake produced by a "D" shape cylinder are studied when local stationary disturbances are placed downstream in the wake (one or two small control cylinders). The control cylinders have for main effect to push away further downstream the maxima of the global mode amplitude (or to increase the formation length). On the other hand and in accordance to the cavity models, it is found that the larger the drag reduction, the larger the size of the recirculation bubble of the "D" cylinder. These results suggest that the efficiency of this passive drag control depends crucially on the role of the global mode instability in the mechanism of the bubble closure.

Key words: global instability, bluff-bodies, drag, incompressible flow.

1. Introduction

The turbulent drag of 2D bluff bodies in incompressible flow at large Reynolds numbers is one of the oldest problem in fluid mechanics that remains one of the most important, for practical reasons and theoretical interest [1]. The underlying physics can be approached by three major ingredients, the steady potential flow with cavity models (see [2] and references therein), the momentum turbulent diffusion (see [3] and references therein) and the global mode instability (referred later as the *BvK* instability) corresponding to the well known Kármán street (see [4] and references therein). The connection between these ingredients has always been one of the best hope to edify a complete theory for bluff body wakes. In the case of natural wakes of different cylinder shape, some empirical [5] and semi empirical [6] fruitful approaches allowed to relate global properties of the wake such as the frequency of the vortex shedding (a major ingredient for the *BvK* instability) to the characteristic size and the pressure of the region of slow fluid motion (major ingredients of the cavity models). Generally, it is found for natural wakes that the lower the drag (or equivalently the higher the base pressure) the lower the shedding frequency and the larger the region of slow fluid motion. However, when wakes are disturbed by the presence of a splitter plate or small secondary cylinder, the opposite can be observed : drag reduction can be associated with an increase of the shedding frequency [7], [8].

In the present work, we study the wake properties of a "D" shape cylinder with one and too local disturbances. The disturbances we consider are small circular cylinders whose positions in space have been optimized to obtain the higher base pressure coefficient of the "D" cylinder (i.e. lower drag). The configuration with one cylinder is similar to cases studied by [9], [10], and [11].

2. Experimental set-up and specific arrangement of control cylinders

The Eiffel type wind tunnel is an open loop air flow facility. The turbulent intensity is less than 0.3% and the homogeneity of the velocity over the $400mm * 400mm$ blowing section is $\pm 0.4\%$. The wake is produced by a symmetric "D" shape cylinder (see figure 1) with a leading face profiled as a semi-circle, and a flat trailing plane at right angles to the flow. The width of the trailing vertical plane is $D = 25mm$. The main flow velocity is $U_0 = 22m/s$, and the Reynolds number of the wake, defined as $Re = U_0 D/\nu \approx 36600$.
The three different flow configurations we studied are shown in figure 1. The first one, denoted $\sharp N$, is the natural wake. The two others have been obtained after an optimization of the base pressure coefficient C_{pb} of the "D" cylinder. For the natural wake, the base pressure coefficient is -0.56. For the second configuration [12] (denoted $\sharp 1$), a small circular cylinder of diameter $d/D = 0.12$ is placed downstream. This control cylinder is a local and steady disturbance to the natural wake of the "D" cylinder. We measured the base pressure versus the position of the control cylinder. The contour map of the isolines of C_{pb} is reported in figure 2(a). Whatever the position, the base pressure is always increased (which is equivalent to a drag reduction), we also find that the wake frequency is always increased. The maxima of base pressure corresponds to maxima of frequency. For configuration $\sharp 1$ we chose to fix the control cylinder at $x_C/D = 0.5$, $y_C/D = 0.6$ where the base pressure coefficient is high, about -0.33. For the third configuration, another small circular cylinder (identical to the previous one) is placed downstream the previous one. Now the second control cylinder is a local disturbance of the previous configuration $\sharp 1$. We measured again the base pressure of the "D" cylinder versus the position of the control cylinder. The contour map of the isolines of C_{pb} is reported in figure 2(b). Again, we find that whatever the disturbance position, the base pressure is always increased, but now the frequency is always decreased compared to that of configuration $\sharp 1$. The maxima of the base pressure corresponds to minima of frequency. We chose to place the second control cylinder at the position $x_C/D = 1.28$, $y_C/D = -0.45$ for which a large base pressure coefficient of $C_{pb} = -0.23$ is obtained. It is worth noticing that if there is only one control cylinder in the wake at this location (see figure 2(a)), the C_{pb} would have increased only to -0.51. The experimental arrangement for the configurations $\sharp N, \sharp 1, \sharp 2$ and dimensions are depicted in figure 1. The pressure distribution around the body is given for the three configurations in figure 3(a). For the Reynolds number considered, the viscous stresses are negligible compared to that of the pressure. Since the pressure distribution are equivalent for the three configurations at the front of the body, the larger the pressure deficit at the rear of the body, the larger the drag exerted on the bluff body. We can then attest for a significant drag reduction, the drag in $\sharp 2$ is lower than $\sharp 1$ that is lower than the natural case $\sharp N$. The main wake characteristics for the three configurations are listed in table 1.
The velocity field is investigated with a PIV set-up and a hot wire probe. In each case, measurements are performed in the plane xOy (see figure 1 and concern the

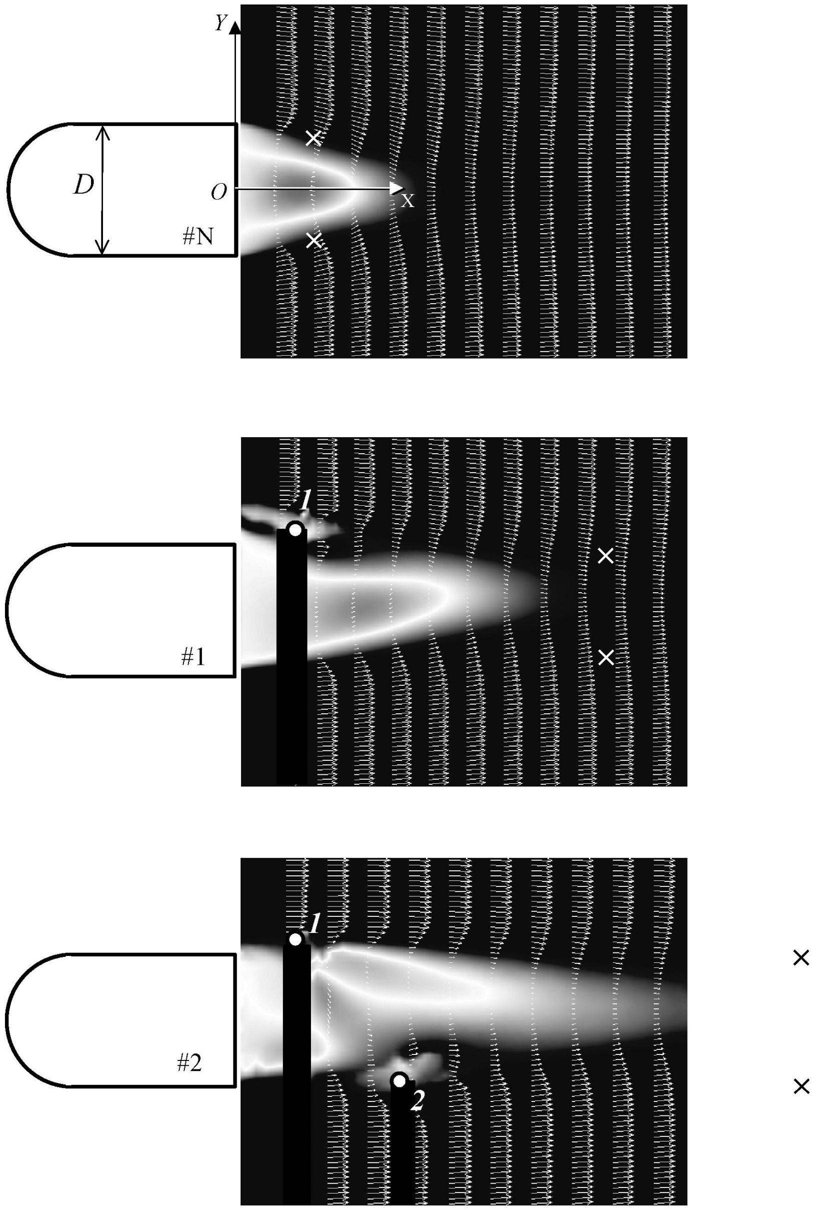

Figure 1. The three different flow configurations. $\sharp N$ is the natural wake, $\sharp 1$ is with one control cylinder and $\sharp 2$ with two control cylinders. The control cylinder labelled (1) is located at $x_C/D = 0.5$, $y_C/D = 0.6$. The control cylinder labelled (2) is located at $x_C/D = 1.28$, $y_C/D = -0.45$. Arrows represent the mean velocity field, the background grayscale is the x-component $< u >$ of the mean velocity field. The white regions correspond to a zero of $< u >$, they enclose regions of negative $< u >$ representative to the back flow. The crosses indicate the positions $(x_G/D,\ y_G/D)$ of the global mode maxima measured from the figure 4.

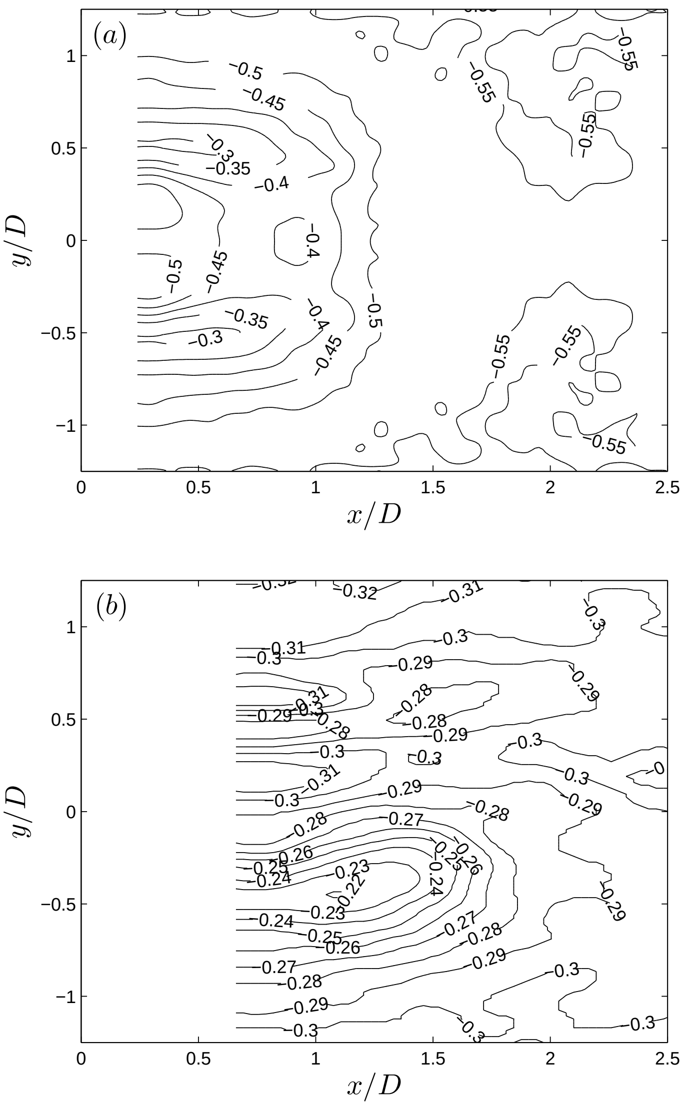

Figure 2. Base pressure coefficient map C_{pb} of the "D" cylinder for (a) one control cylinder at the various positions $(x/D, y/D)$ and (b) one control cylinder fixed at $(x/D = 0.5, y/D = 0.6)$ and the other at various positions $(x/D, y/D)$.

Config.	$-C_{pb}$ (± 0.02)	$St = \frac{f_0 D}{U_0}$	$A_{max}(f_0)(m/s)$	x_G/D, y_G/D (± 0.05)
$\sharp N$	0.56	0.234	2.86	0.6, 0.42
$\sharp 1$	0.33	0.250	1.36	2.8, 0.42
$\sharp 2$	0.23	0.212	1.78	4.25, 0.5

Table 1. Main characteristics of the wake for the 3 configurations.

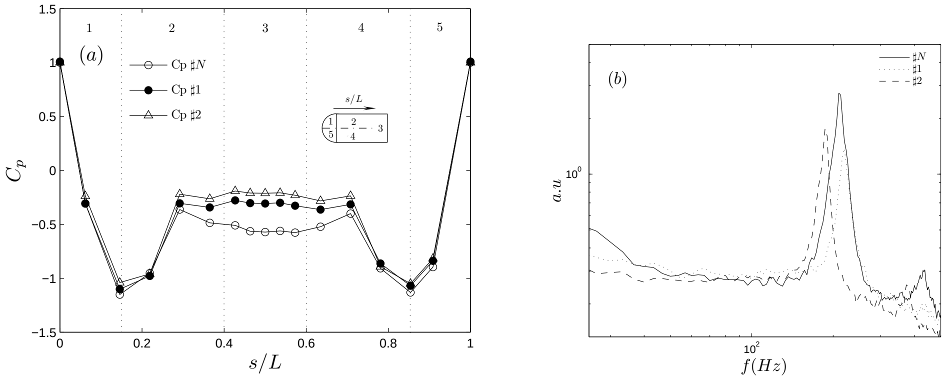

Figure 3. (a) : pressure coefficient distribution around the main body for the 3 configurations. (b) : amplitude spectrum of the velocity measured with the hot wire probe for the 3 configurations. Each spectrum corresponds to the locations (measured from figure 4 and localized by crosses in figure 1) in the wake where the amplitude at the fundamental frequency of the BvK instability is maximum.

u and v components of the velocity field only. For the hot wire measurements, the wire is oriented such a way to be essentially sensitive to the modulus $u^2 + v^2$. We will call $U = \sqrt{u^2 + v^2}$, the velocity measured by the wire probe. At each point in space (the resolution is $\delta x/D = 0.24$ and $\delta y/D = 0.16$), the probe signal is recorded during $120s$ at a sampling frequency of $5kHz$.

3. Results

The mean flows, obtained by averaging in time the PIV velocity fields, are shown in figure 1. Comparing the vector fields, We can see that the mean momentum deficit in the wake is increased by the presence of the control cylinders. From the pressure distribution measurements for each configuration (figure 3(b), we observe that the larger the deficit momentum the lower $-C_{pb}$ (or equivalently the drag). In the close wake, the drag is related to the strong pressure gradient and not to the momentum deficit as it is the case in the far wake [3]. The characteristic length of the recirculation bubble, revealed by the region of negative $< u >$ component in figure 1 is increased as the drag is reduced. Both observations about the momentum deficit and the bubble length are qualitatively consistent with the cavity models [2], [13]. In this model, the larger the dead zone region (i.e. the region of the slow fluid motion), the lower the $-C_{pb}$ or equivalently the drag. The recirculation bubble that becomes asymmetric with one control cylinder split into two parts with two control cylinders.

Spectral measurements in the wake indicate that the flow is synchronized for the three configurations. Whatever the position in the wake, we find a clear global frequency whose magnitudes are $211Hz$ for the natural wake, $220Hz$ with one control cylinder and $186Hz$ for two control cylinders (see spectra in figure 3(b)). The corresponding Strouhal numbers based on the characteristic length D are displayed in table 1. We extracted the amplitude of the peak corresponding to the fundamental frequency (mode 1) and to the harmonic (mode 2). This peak's amplitude measured in space, say $A_{f_0}(x, y)$, defines the global mode envelope of the mode 1 [14]. This

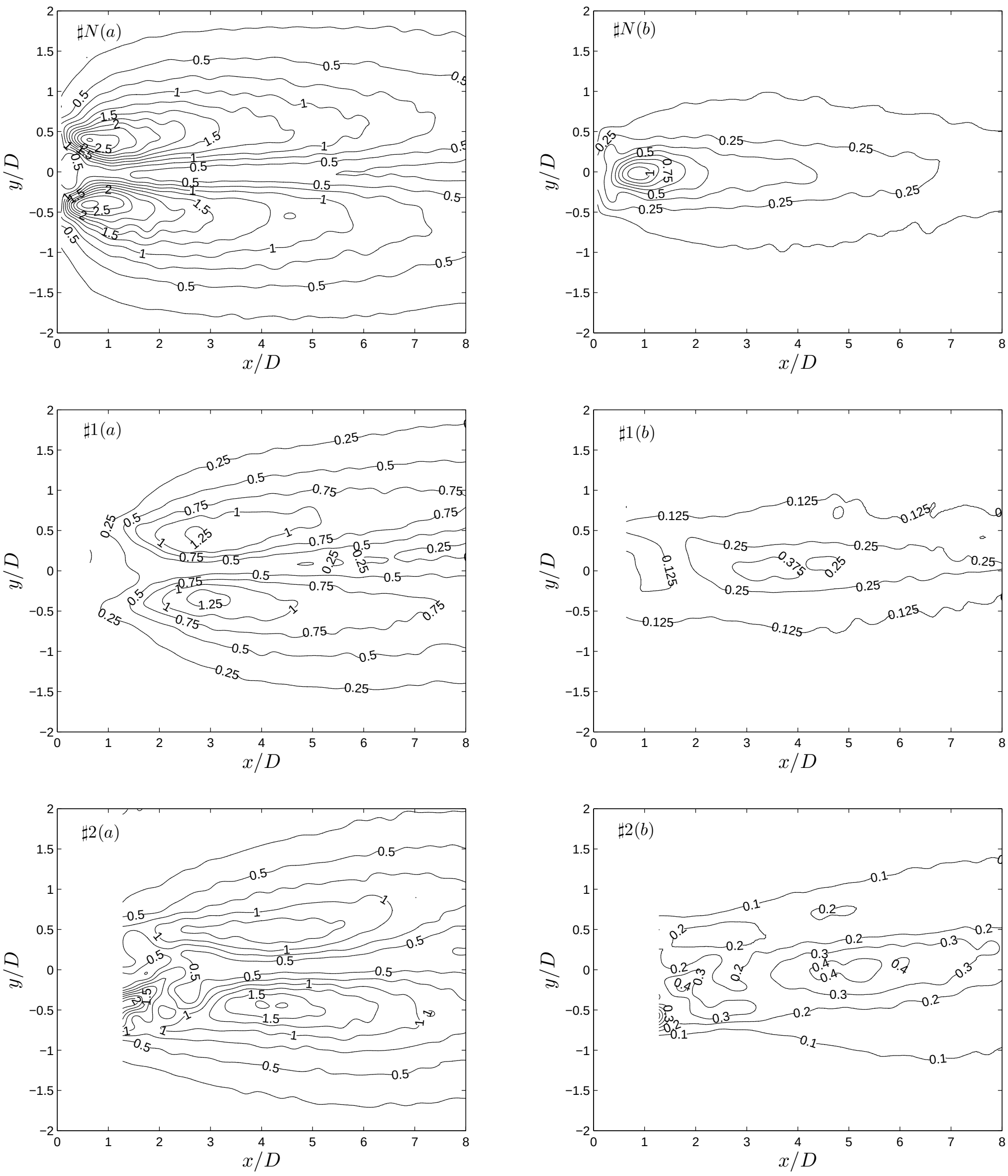

Figure 4. Pressure coefficient distribution around the main body for the three configurations.

envelope is characteristic to the underlying global instability [4]. The global mode envelope for the fundamental frequency and its harmonic are shown in figure 4. For the natural wake $\sharp N$, two maxima of magnitudes about $A_{max}^{\sharp N} = 2.86 m/s$ are found very close to the rear of the bluff-body at $x_G/D = 0.6D$ and symmetrically located at $y_G/D = \pm 0.42D$ (figure 4(a)). We can see in figure 1 that the global mode maxima (found in figure 4(a) and displayed by the crosses in figure 1 for configuration $\sharp N$) are situated upstream the closure of the re-circulation bubble. For the controlled wake in configuration $\sharp 1$, the maxima are significantly damped by a factor 2, their magnitudes are now about $A_{max}^{\sharp 1} = 1.36 m/s$ and located much further downstream in the wake at $x_G/D = 2.8$. Now, the maxima are situated downstream the closure of the re-circulation bubble (see figure 1). Their positions are still rather symmetrically located as for the natural wake at positions $y_G/D = \pm 0.42D$. With the second control cylinder, the maxima are again shifted downstream at about $x_G/D = 4.25$ and further downstream the closure of the recirculation bubbles (see figure 1). The positions are still rather symmetrically located but their separating distance is increased compared to cases $\sharp N$ and $\sharp 1$ since now $y_G/D = \pm 0.5D$. The magnitude of the maxima is increased compared to that of the case with one cylinder, $A_{max}^{\sharp 2} = 1.78 m/s$ but remains lower than the natural case. The study of the global mode envelope at the harmonic frequency in figure 4(b) leads to same conclusions.

4. Discussions and conclusion

There are only few attempts [9],[10] to understand the effect of drag reduction due to a small control cylinder placed in the wake of a larger cylinder. From our point of view, the first control cylinder in configuration $\sharp 1$ "forces" the shear layer to roll up further downstream. This is a similar effect to that observed in the case of "wake interference" in [6]. The consequence is an increase of the recirculation bubble and, in accordance to the cavity model [13], a higher base pressure (or equivalently a lower drag). With the second cylinder, the recirculation bubble split into two parts, but the region of slow fluid motion is larger than the previous cases. The drag reduction mechanism seems to be again in agreement with the cavity model.
Although the relationship between the size of the slow fluid region and the base pressure coefficient seems rather clear, the corresponding modification of the *Bvk* instability deserves attention. As the region of slow fluid motion increases, the maxima of the global mode are shifted downstream (it is similar to an increase of the formation length as defined in [5]). Both effects are consistent and related to a delay in the instability. However the frequency modification are opposite (see table 1). There is then no direct relation between the base pressure and the *Bvk* instability. It is worth noticing that a *Bvk* global mode instability coupling too shear layers can be obtained without any low pressure between them [15]. However, it seems obvious that the global mode plays an important role in the closure of the region of slow fluid motion (and then to the drag) for the natural wake. Actually, in that case the maxima of the global mode occur before the closure (see figure 1). For the two other configurations, with passive control, the maxima occur much further downstream the closure of the recirculation bubble (see figure 1) and one may wonder whether the global mode is the only relevant mechanism for the closure. Actually, the opposite shears produced by the "D" cylinder are strongly disturbed by the control cylinders implying flow deviations and increase of the turbulent mixing.

Both effect could be responsible for the closure.
In conclusion, since the main effect of this passive control with small cylinders is to shift downstream the global mode envelop, our results suggest that its efficiency to reduce drag depends on the role of the global mode in the closure mechanism of the recirculation bubble.
Another property that we would like to study is the reversed behavior between the wake frequency and the global mode amplitude. We observed that an increase of the frequency is always associated to a decrease of the amplitude and vice versa with no exception (whatever the position and the number of disturbances in the wake). The effect is certainly a manifestation of the budget equation of the flux of circulation per unit of length primarily created by the ”D” shape cylinder.

References

[1] Roshko, A. 1993 Perspectives on bluff body aerodynamics. *J. Fluid. Wind Eng. and Ind. Aero.* **49**, 79-100.

[2] Wu Y.T. 1978 Cavity and wake flows. *Ann. Rev. Fluid. Mech.* **4**, 243-284.

[3] Pope S.B. 2000 Turbulen flows. *Cambridge university press.*

[4] Chomaz, J.-M. 2005 Global instabilities in spatially developing flows: non normality and nonlinearity. *Ann. Rev. Fluid. Mech.* **37**, 357-392.

[5] Gerrard, J.H. 1966 The mechanics of the formation region of vortices behind bluff bodies *J. Fluid. Mech.* **25**, 401-413.

[6] Roshko, A. 1954 On the drag and shedding frequency of 2D bluff bodies. *NACA Tech. Note 3169.*

[7] Bearman P.W., 1965 Investigation of the flow behind a two-dimensionnal model with a blunt trailing edge and fitted splitter plates *J. Fluid. Mech.* **21**, 241.

[8] Sakamoto H., Tan K. & Haniu, H. 1991 An optimum suppression of fluid forces by controlling a shear layer separated from a square prism. *J. Fluid. Eng.* **113**, 183-189.

[9] Sreenivasan, K. R. & Strykowski, P.J. 1990 On the formation and suppression of vortex shedding at low Reynolds number. *J. Fluid. Mech.* **218** 71–108.

[10] Mittal, S. & Raghuvanshi, A. 2001 Control of vortex shedding behind circular cylinder for flows at low Reynolds numbers. *Int. J. Numer. Mech. Fluids* **35**, 421-447.

[11] Dalton, C., Xu, Y. & Owen, J.C. 2001 The suppression of lift on a circular cylinder due to vortex shedding at moderate Reynolds numbers. *J. Fluids Struc.* **15**, 617-628.

[12] Thiria B., Beaudoin J.-F., and Cadot O. 2007 Passive drag control of a blunt trailing edged cylinder. *Journal of fluid and structures, submitted.*

[13] Riabouchinsky D. 1920 On steady fluid motions with free surface. *Proc. London Math. Soc. Ser. 2* **19**, 206-215.

[14] Zielinska, B. & Wesfreid, J.E. 1995 On the spatial structure of global modes in wake flow. *Phys. Fluids.* **7**, 1418.

[15] Abernnathy, F. H. & Kronauer, R.E. 1962 The formation of vortex streets. *J. Fluid. Mech.* **13** 1–20.